The effect of nonzero viscosity ratio on the stability of fingers and bubbles in a Hele–Shaw cell

S. Tanveer
Department of Mathematics, Virginia Polytechnic Institute and State University, Blacksburg, Virginia 24061-4097

P. G. Saffman
Department of Applied Mathematics, California Institute of Technology, Pasadena, California 91125

(Received 7 March 1988; accepted 17 June 1988)

The linear stability of a steadily moving bubble or a finger in a Hele–Shaw cell is considered in the case when gravity and the ratio between the viscosities of the less and more viscous fluids are nonzero. The effect of gravity is easily incorporated by a transformation of parameters introduced previously by Saffman and Taylor [Proc. R. Soc. London Ser. A **245**, 312 (1958)] for the steady flow, which makes the time-dependent flows with and without gravity equivalent. For the nonzero viscosity ratio, the transformation of parameters introduced by Saffman and Taylor also makes steady finger and bubble flows with nonzero and zero viscosity ratios equivalent. However, for the unsteady case, there is no such equivalence and so a complete calculation is carried out to investigate the effect of the nonzero viscosity ratio on the stability of fingers and bubbles. The incorporation of the finite viscosity ratio is found not to qualitatively alter the linear stability features obtained in earlier work for the zero viscosity ratio, although there are quantitative differences in the growth or decay rate of various modes. For any surface tension, numerical calculation suggests that the McLean–Saffman branch of bubbles [Phys. Fluids **30**, 651 (1987)] of arbitrary size is stable, whereas all the other branches are unstable. For a small bubble that is circular, the eigenvalues of the stability operator are found explicitly. The previous analytic theory for the stability of the finger in the limit of zero surface tension is extended to include the case of the finite viscosity ratio. It is found that, as in the case of bubbles, the finite viscosity ratio does not alter qualitatively any of the features obtained previously for the zero viscosity ratio.

I. INTRODUCTION

Two-phase flow in a Hele–Shaw cell has attracted much attention in recent years in view of its relation to a multitude of problems in oil reservoir engineering and dendritic crystal growth and to problems of pattern selection and phase transition. Reviews by Saffman,[1] Bensimon *et al.*,[2] and Homsy[3] summarize the state of affairs as of two years ago. Since then, there has been a fair amount of progress in the understanding of the selection[4–12] and stability[4,13–18] of fingers and bubbles. It is now known that surface tension selects a discrete set of symmetric fingers and bubbles out of a continuum of solutions where both the velocity and the distance of the finger or bubble centroid from the channel centerline remain arbitrary. For small surface tension, the selection mechanism is accounted for by transcendentally small terms in the perturbation about the zero surface tension solutions for symmetric or nonsymmetric fingers or bubbles.[19,20,9,21] It is also known now that only one solution corresponding to the largest relative velocity of the finger or bubble is stable, while others are unstable for any surface tension. These results are based on simplified boundary conditions at the finger boundary, where the effect of the thin film left behind the advancing interface is totally neglected and the transverse curvature is assumed to be a constant. It is also assumed in the simplified theory that there is no gravity and that the viscosity of the less viscous fluid is zero.

There remain significant discrepancies between experiment and predictions of the simplified theory. For the case of a finger, the experiments[19,22] give a different dependence of the finger width on the capillary number than predicted by theory.[23] Further, experiment also shows that for very large capillary number, the finger is unstable, in disagreement with the conclusions of the simplified theory. More realistic boundary conditions have been developed[24,25] for the case of a steady finger that account for the thin film left behind by the advancing finger. Recent calculations of finger width for different capillary number using these[26,27] boundary conditions are in good agreement with experiment.

For the case of a bubble, the disagreement between simplified theory[8,9,20] and experiment[28,29] is quite large and more realistic boundary conditions are yet to be developed. It is to be noted that the wetting properties of advancing and receding interfaces are quite different; this has to be accounted for in developing proper boundary conditions for a bubble.

The stability of fingers and bubbles with boundary conditions incorporating the thin film effect remains unexplored and may account for most of the discrepancy with experiments. There are other mechanisms that may explain the observed instability. One is the nonlinear interaction of the modes[2,30] that have been explored for the simplified set of boundary conditions. Numerical evidence[2] suggests that for the simplified theory, the critical amplitude for the onset of instability goes to zero exponentially as the surface tension tends to zero. However, it is unclear that this accounts for most of the experimentally observed instability. Given the delicate role of surface tension (through transcendentally

 0031-9171/88/113188-11$01.90

small terms) in the linear stability analysis[16] based on simplified boundary conditions, the question arises whether finite viscosity can destabilize fingers and bubbles for small surface tension and account for experimentally observed instability. This question is addressed here.

The purpose of this paper is to explore the effect of the finite viscosity ratio on the stability of fingers and bubbles. The fluids are also allowed to have differing densities and gravity is assumed in the direction opposite to the advance of the finger. However, the thin film effect and the variation of transverse curvature are both ignored. The effect of gravity on the linear stability analysis is trivially incorporated since there exists a transformation of parameters that makes the problem with and without gravity equivalent. In the context of the steady-state finger, this transformation was found originally by Saffman and Taylor,[19] who showed that gravity and finite viscosity ratio only change the effective surface tension and finger velocity in the problem with zero gravity and viscosity ratio. However, there is no such transformation for the time-dependent problem for the finite viscosity ratio and so a complete calculation is carried out. For steady bubbles of small size that are circular, it is possible to explicitly calculate all the modes; we find that for any surface tension, the steady bubble is stable just as for the zero viscosity ratio. For bubbles of arbitrary size, we modify the previous numerical method[17] to account for the flow inside the bubble and find that even for the nonzero viscosity ratio, the bubbles that correspond to the fingers first calculated by McLean and Saffman[23] in the limit of large area remain stable for any surface tension that is not too small. The numerical method for the calculation of the eigenvalues of the stability operator break down for very small surface tension because more and more terms are necessary in the truncation of a basis representation for accurate eigenvalue calculations as the surface tension tends to zero. However, from extrapolation of the eigenvalues to the zero surface tension, as well as from the results of the analytic theory for the finger developed here for the nonzero viscosity ratio for the limit of zero surface tension, it is safe to conclude that bubbles as well as fingers remain stable for nonzero surface tension for the McLean–Saffman branch. The Romero–Vanden-Broeck branches of finger[31,32] and bubbles[9,17] remain unstable just as for the zero viscosity ratio. However, the growth and decay rates of the modes are modified by the finite viscosity ratio effect.

The extension of the analytic theory for the linear stability of the finger developed here for the nonzero viscosity ratio rests on some assumptions that have not been verified directly. However, there is indirect evidence that the assumptions are correct. For the Romero–Vanden-Broeck branches, the numerical calculations of the growth rates of the unstable eigenmodes for large bubbles extrapolated to zero surface tension agree with the prediction of the analytic theory for the finger, as they should, since the unstable eigenmodes only affect the front of the bubble and are unaffected by a further increase in bubble size. Further, the prediction of power law dependence of the growth rate as a function of surface tension is found to be in correspondence with numerics.

II. FORMULATION OF THE TIME-DEPENDENT PROBLEM

Figure 1 shows the Hele–Shaw geometry in the lateral $\tilde{x}$-$\tilde{y}$ plane in the laboratory frame. Gravity denoted by g acts in the negative $\tilde{x}$ direction opposite to the direction of the advance of the finger or bubble. In the steady case the velocity of the bubble or the finger is denoted by $\tilde{U}$, whereas the velocity of the displaced fluid as $\tilde{x}\to\infty$ is V. From the condition that the fluid flow is incompressible, it is easy to see that the fluid velocity for the finite bubble at $\tilde{x}=-\infty$ is V. The densities and viscosities of the displaced and displacing fluids are ρ,μ and ρ_v,μ_v, respectively. In the Hele–Shaw cell approximation, the averaged velocity over the narrow gap direction, which is a function of $\tilde{x}$ and $\tilde{y}$ and time $\tilde{t}$, is the gradient of a potential, which for fluid outside the finger or bubble is related to the pressure $\tilde{p}$ (see Saffman and Taylor[19] for details) by

$$\tilde{\phi}=-(b^2/12\mu)(\tilde{p}+\rho g\tilde{x})\,, \tag{1}$$

where b is the channel gap. For the fluid inside, the pressure $\tilde{p}_v$ is related to the velocity potential $\tilde{\phi}_v$ by the relation

$$\tilde{\phi}_v=-(b^2/12\mu_v)(\tilde{p}_v+\rho_v g\tilde{x})\,. \tag{2}$$

From the incompressibility condition, we have

$$\nabla^2\tilde{\phi}=0 \tag{3}$$

and

$$\nabla^2\tilde{\phi}_v=0\,. \tag{4}$$

The boundary condition at $\tilde{x}=+\infty$ and $\tilde{\phi}$ is

$$\tilde{\phi}=V\tilde{x}+O(1)\,. \tag{5}$$

For the bubble, from continuity, Eq. (5) holds at $\tilde{x}=-\infty$ as well. On the walls, $\tilde{\psi}$,the harmonic conjugate of $\tilde{\phi}$, satisfies the boundary condition

$$\tilde{\psi}=\pm Va \tag{6}$$

on $\tilde{y}=\pm a$, where a denotes the half-width of the cell. For the finger, as $\tilde{x}\to-\infty$, the flow inside the finger satisfies the boundary condition

$$\tilde{\phi}_v=\tilde{U}\tilde{x}+O(1)\,, \tag{7}$$

where it is assumed that in a time-dependent problem such as in the steady state, the finger boundary is asymptotically parallel to the walls and the relative finger width λ is independent of time. Thus we will not be considering the class of disturbances that change the width of the steady finger. We now discuss the interfacial boundary conditions. Neglecting the effect of the thin film and the variation of transverse curvature, the pressure condition reduces to

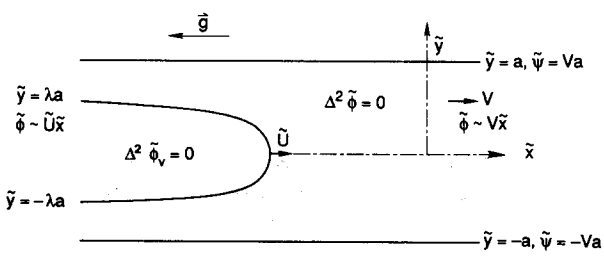

FIG. 1. The Hele–Shaw cell geometry for an advancing finger in the physical $\tilde{x}$-$\tilde{y}$ plane.

$$\mu\tilde{\phi} - \mu_v\tilde{\phi}_v = (b^2T/12)\tilde{\kappa} - (b^2/12)(\rho - \rho_v)g\tilde{x} + \text{const}, \tag{8}$$

where $\tilde{\kappa}$ is the lateral curvature and the constant on the rhs of (8) can depend on time. From (7) and (8) it follows that as $\tilde{x} \to -\infty$,

$$\tilde{\phi} = [-(b^2/12\mu)(\rho - \rho_v)g + (\mu_v/\mu)\tilde{U}]\tilde{x} + O(1). \tag{9}$$

The kinematic conditions at the interface for the general time-dependent problem can be expressed as

$$\tilde{\psi} = \tilde{\psi}_v, \tag{10}$$

$$\frac{\partial\tilde{F}}{\partial\tilde{t}} + \frac{\partial\tilde{\phi}}{\partial\tilde{x}}\frac{\partial\tilde{F}}{\partial\tilde{x}} + \frac{\partial\tilde{\phi}}{\partial\tilde{y}}\frac{\partial\tilde{F}}{\partial\tilde{y}} = 0, \tag{11}$$

where $\tilde{F}(\tilde{x},\tilde{y},\tilde{t}) = 0$ describes the interface and the stream-function $\tilde{\psi}_v$ is the harmonic conjugate of $\tilde{\phi}_v$ inside the finger or bubble.

In the steady case, the fluid inside the finger or bubble has a constant velocity $\tilde{U}$ and therefore

$$\tilde{\phi}_v = \tilde{U}\tilde{x} \equiv \tilde{\phi}_{vs}. \tag{12}$$

The mathematical problem is then reduced to solving for the velocity potential $\tilde{\phi} = \tilde{\phi}_s$ outside the finger or bubble, with the boundary conditions (8)–(10) reducing to two boundary conditions on the interface:

$$\tilde{\psi}_s = \tilde{U}\tilde{y} \tag{13}$$

and

$$\mu\tilde{\phi}_s = [\mu_v\tilde{U} - (b^2/12)(\rho - \rho_v)g]\tilde{x} + (b^2T/12)\tilde{\kappa}. \tag{14}$$

Saffman and Taylor[19] showed that the above steady-state problem is equivalent to a flow with $\mu_v = 0$ and $g = 0$, where the effective values of T, μ, and $\tilde{U}$ are transformed to a different set of values. We now consider the general time-dependent problem and carry out such a transformation. We also nondimensionalize our variables and move to a frame where the steady finger or bubble is at rest.

Consider the change of variables

$$x = (\tilde{x} - \tilde{U}\tilde{t})/a, \tag{15}$$

$$y = \tilde{y}/a, \tag{16}$$

$$t = \tilde{t}V/a, \tag{17}$$

$$\psi = (\tilde{\psi} - \tilde{U}\tilde{y})/a(V - \hat{U}), \tag{18}$$

$$\phi = (\tilde{\phi} - \tilde{U}\tilde{x})/a(V - \hat{U}), \tag{19}$$

$$\psi_v = (\tilde{\psi}_v - \tilde{U}\tilde{y})/a(V - \hat{U}), \tag{20}$$

$$\phi_v = (\tilde{\phi}_v - \tilde{U}\tilde{x})/a(V - \hat{U}), \tag{21}$$

$$\hat{U} = (\mu_v/\mu)\tilde{U} - (b^2/12\mu)(\rho - \rho_v)g, \tag{22}$$

$$\tilde{F}(\tilde{x},\tilde{y},\tilde{t}) = F(x,y,t). \tag{23}$$

If we set

$$U = (\tilde{U} - \hat{U})/(V - \hat{U}), \tag{24}$$

then each of ϕ and ϕ_v is harmonic in the variables x and y outside and inside the bubble (or finger), respectively. The boundary condition at $x = +\infty$ is

$$\phi = -(U - 1)x \tag{25}$$

and on the walls at $y \pm 1$, it is

$$\psi = \mp(U - 1). \tag{26}$$

The pressure condition on the interface is

$$Ux + \phi - \phi_v\alpha = \mathscr{B}\kappa, \tag{27}$$

where any possible constants on the rhs of (27) are absorbed in ϕ, κ is the nondimensional curvature, and

$$\alpha = \mu_v/\mu, \tag{28}$$

$$\mathscr{B} = b^2T/12\mu(V - \hat{U})a^2. \tag{29}$$

The kinematic conditions are

$$\psi_v = \psi, \tag{30}$$

$$\frac{\partial F}{\partial t} + \frac{\partial\phi}{\partial x}\frac{\partial F}{\partial x} + \frac{\partial\phi}{\partial y}\frac{\partial F}{\partial y} = 0. \tag{31}$$

An additional boundary condition is required on ϕ_v at $x = -\infty$ in the case of a finger. From (7) and (21), it is clear that without loss of generality

$$\phi_v = 0 \tag{32}$$

at $x = -\infty$. We also note from (27) and (32) that for the finger as $x \to -\infty$, $\phi \sim -Ux$. From the continuity of fluid flow between $x = +\infty$ and $-\infty$, it follows from this and (25) that $U(1 - \lambda) = U - 1$ and so $\lambda = 1/U$ for the finger. Thus $U > 1$ for the finger. For the bubble, the zero surface tension solutions[20,9] require $U > 1$; we suspect that this is the case at least for our[33] boundary conditions although we are unable to prove it.

For the steady state, there is no time dependence and ϕ_v is identically zero, as can be seen from (12) and (21). In that case, the conditions (25)–(27) and (30)–(32) do not involve μ_v or g. These parameters enter into the problem only through U and $\mathscr{B}$. This observation was originally made by Saffman and Taylor.[19] We note that for μ_v and g unequal to zero, U is no longer the actual bubble or finger velocity relative to flow at infinity. It is the effective bubble velocity for the equivalent $\alpha = 0$ and $g = 0$ steady flow.

For the time-dependent problem, once again g does not explicitly appear in the equations, except through the parameters U and $\mathscr{B}$. However, the finite viscosity ratio α appears in the equation explicitly. It is clear then that the stability problem of nonzero viscosity ratio requires solving for both the harmonic functions ϕ and ϕ_v outside and inside the finger or bubble.

III. SMALL BUBBLE ANALYSIS

In the limit when the bubble dimension is small compared to the width of the cell, yet large compared to the cell gap so that Hele–Shaw cell approximation is valid, the effect of the walls can be ignored in our equations and the steady bubble corresponding to the McLean–Saffman branch of solution is circular[8] and has $U = 2$. We consider the stability of this steady bubble solution to infinitesimal disturbances that preserve the flux of fluid at infinity. For convenience, we introduce a new set of scaled variables:

$$\bar{x} = xa/R, \tag{33}$$

$$\bar{y} = ya/R, \tag{34}$$

$$\bar{\phi} + i\bar{\psi} = (\phi + i\psi)a/R, \tag{35}$$

$$\bar{\phi}_v + i\bar{\psi}_v = (\phi_v + i\psi_v)a/R, \tag{36}$$

where R is the radius of the small circular bubble. The dynamic boundary condition (27) then reduces to

$$\bar{\phi} + 2\bar{x} - \alpha\bar{\phi}_v = \mathscr{C}\bar{\kappa}, \tag{37}$$

where $\bar{\kappa} = \kappa R/a$ and

$$\mathscr{C} = \mathscr{B}a^2/R^2. \tag{38}$$

On the disturbed bubble boundary

$$r = 1 + F(\theta,t), \tag{39}$$

where r is the radial distance from the bubble center and θ is the angle with respect to the positive $\bar{x}$ axis, the kinematic conditions reduce to

$$\bar{\psi}_v = \bar{\psi}, \tag{40}$$

$$\frac{D}{Dt}[r - 1 - F(\theta,t)] = 0, \tag{41}$$

where D/Dt refers to the comoving derivative. The boundary condition on $\bar{\phi}$ at ∞ is

$$\bar{\phi} \sim -\bar{x} + O(1/r), \tag{42}$$

where we assume that there are no logarithmic terms (sources). We decompose the velocity potential

$$\bar{\phi} = \bar{\phi}_0(r,\theta) + \bar{\phi}_1(r,\theta,t), \tag{43}$$

where $\bar{\phi}_0$ is the exterior potential corresponding to the steady flow and is

$$\bar{\phi}_0 = -(r + 1/r)\cos\theta. \tag{44}$$

Linearizing the equations of motion about the steady state and assuming the bubble boundary to be analytic, we can shift the boundary conditions back to the original circular boundary by standard expansion. Assuming an $e^{\sigma t}$ time dependence for the dependent variables, one finds that the equations determining linear stability are given by the following boundary conditions on $r = e^{i\theta}$:

$$\frac{\partial\bar{\phi}_1}{\partial r} - 2\cos\theta F = \sigma F + 2\sin\theta\frac{\partial F}{\partial\theta}, \tag{45}$$

$$\frac{\partial\bar{\phi}_v}{\partial r} = \sigma F, \tag{46}$$

$$2\cos\theta F + \bar{\phi}_1 - \alpha\bar{\phi}_v = -\mathscr{C}\left(F + \frac{\partial^2 F}{\partial\theta^2}\right). \tag{47}$$

It is easy to see from the boundary conditions (45)–(47) that any eigenfunctions comprising the triple $(\bar{\phi}_1,\bar{\phi}_v,F)$ are either even or odd functions of the angular variable θ, corresponding to symmetric or antisymmetric disturbances. In fact, this result carries over to arbitrary size bubbles that are symmetric about the channel centerline. For symmetric disturbances, we write

$$F = \sum_1^\infty a_n \cos n\theta, \tag{48}$$

$$\bar{\phi}_1(r,\theta) = \sum_0^\infty b_n r^{-n}\cos n\theta, \tag{49}$$

and, using (46),

$$\bar{\phi}_v(r,\theta) = \sum_1^\infty \frac{\sigma a_n}{n} r^n \cos n\theta. \tag{50}$$

Substituting into (45) and (47), we find the following recurrence relation:

$$a_2 = (1 + \alpha)\sigma a_1/2 \tag{51}$$

and, for $n \geqslant 2$,

$$a_{n+1} = (1/2n)[(1 + \alpha)\sigma + \mathscr{C}n(n^2 - 1)]a_n. \tag{52}$$

Now, if $\mathscr{C}$ is nonzero, it is clear from the recurrence relation (52) that in general a_n grows with n for large n. This is unacceptable since the infinite series representation in (48) will not be convergent. Thus the series in (48) must truncate, implying that the nonzero eigenvalues form a discrete set of real negative values given by $\{\sigma_m\}$, where

$$\sigma_m = -[\mathscr{C}/(1 + \alpha)]m(m^2 - 1), \tag{53}$$

with the integer m ranging from 2 to ∞. Thus the bubble is stable when any amount of surface tension is introduced. From (53), it is clear that the decay rate of the disturbance is only affected by a multiplicative constant by the nonzero viscosity ratio.

Now, we consider antisymmetric disturbances. Then

$$F = \sum_1^\infty a_n \sin n\theta, \tag{54}$$

$$\bar{\phi}_1(r,\theta) = \sum_1^\infty b_n r^{-n}\sin n\theta, \tag{55}$$

$$\bar{\phi}_v(r,\theta) = \sum_1^\infty \frac{\sigma a_n}{n} r^n \sin n\theta. \tag{56}$$

Substituting back into (45) and (47), we obtain the same recurrence relation (52) for a_n, where it is now valid for $n \geqslant 1$. Thus we find that, as in the case of symmetric disturbances, any amount of surface tension stabilizes the bubble even for nonzero α.

IV. FORMULATION FOR NUMERICAL DETERMINATION OF BUBBLE STABILITY

We modify the formulation given in Sec. IV of Tanveer and Saffman[17] to include the effect of the finite viscosity ratio; for the most part, the procedure is about the same as the one described in that paper. However, for clarity, we will describe all the steps again. As before, the work plane, called the ζ plane, is chosen to be the annular region between concentric circles, as shown in Fig. 2. In this case, no flow symmetry is assumed and the flow region in the physical region outside the bubble and between the two walls is mapped to the annular region in the ζ plane such that $z = -\infty$ is mapped to $\zeta = \tilde{\rho}$ and $z = +\infty$ is mapped to $\zeta = \tilde{\rho}e^{i\tilde{\beta}}$. The bubble boundary corresponds to the unit circle in the ζ plane and the cell walls correspond to the circle of radius $\tilde{\rho}$. In general $\tilde{\rho}$ and $\tilde{\beta}$ are functions of time. We decompose the mapping function $z(\zeta)$ into

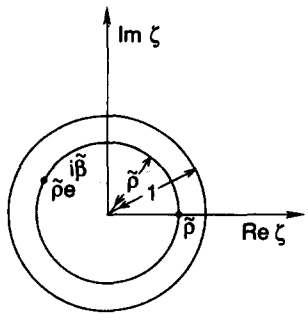

FIG. 2. The ζ plane as defined in Sec. IV. Here, $z = -\infty$ and $z = +\infty$ are mapped to $\zeta = \tilde{\rho}$ and $\tilde{\rho}e^{i\tilde{\beta}}$, respectively.

$$z(\zeta) = z_0(\zeta,\tilde{\rho},\tilde{\beta}) + f(\zeta,\tilde{\rho}) + \tilde{z}_1(\zeta,t)\,, \tag{57}$$

where z_0 is now defined as

$$z_0 = \frac{-i(\pi-\tilde{\beta})}{\pi} + \frac{2}{\pi}\log\left(e^{-i\tilde{\beta}/2}\frac{\theta_1[(-i/2)\ln\zeta + (i/2)\ln\tilde{\rho},\tilde{\rho}^2]}{\theta_1[(-i/2)\ln\zeta - \tilde{\beta}/2 + (i/2)\ln\tilde{\rho},\tilde{\rho}^2]}\right) + \frac{2(U-2)}{\pi U}\log\left(e^{i\tilde{\beta}/2}\frac{\theta_1[(-i/2)\ln\zeta - (i/2)\ln\tilde{\rho},\tilde{\rho}^2]}{\theta_1[(-i/2)\ln\zeta - \tilde{\beta}/2 - (i/2)\ln\tilde{\rho},\tilde{\rho}^2]}\right), \tag{58}$$

where the second argument of the elliptic θ_1 function is its nome, usually denoted by q. For efficient numerical evaluation of θ_1, it is convenient to use the rapidly convergent representation

$$\theta_1(s,q) = 2q^{1/4}\sum_{n=0}^{\infty}(-1)^n q^{n(n+1)}\sin(2n+1)s\,. \tag{59}$$

The function $f(\zeta,\tilde{\rho})$ is dependent on time t only through $\tilde{\rho}$. When $\tilde{\rho}=\rho$, the steady-state value f is determined by the boundary conditions $\mathrm{Im}\,f=0$ on $|\zeta|=\rho$ and

$$U\,\mathrm{Re}\,f = \mathscr{B}\kappa_s \tag{60}$$

on $\zeta = e^{i\nu}$, where κ_s is the steady-state curvature. Now, f is conveniently expressible as a Laurent series:

$$f(\zeta,\rho) = a_0 + \sum_{n=1}^{\infty}(a_n\zeta^n + a_n\rho^{2n}\zeta^{-n})\,, \tag{61}$$

where the coefficients a_n are all real; these have been determined previously.[9] The complex velocity potential is decomposed into

$$W = W_0(\zeta,\tilde{\rho},\tilde{\beta}) + \tilde{W}_1(\zeta,t) + i[(U-1)/\pi](\pi-\tilde{\beta})\,, \tag{62}$$

where

$$W_0 = -2\frac{(U-1)}{\pi}\log\left(\frac{\theta_4[(-i/2)\ln\zeta,\tilde{\rho}]}{\theta_4[(-i/2)\ln\zeta - \tilde{\beta}/2,\tilde{\rho}]}\right) \tag{63}$$

and the second argument of the elliptic θ_4 function is its nome. For efficient numerical evaluation of this function, it is convenient to use the following rapidly convergent series representation:

$$\theta_4(s,q) = 1 + 2\sum_{n=1}^{\infty}(-1)^n q^{n^2}\cos 2ns\,. \tag{64}$$

For the steady-state problem $\tilde{W}_1$ and $\tilde{z}_1$ are each equal to zero. Further, for the steady state, $\tilde{\beta}=\pi$ and $\tilde{\rho}=\rho$, which is a characteristic of the size of the bubble. Inserting (57) and (62) into Eq. (27), the dynamic boundary condition is

$$\tilde{\phi}_1 + U\tilde{x}_1 - \alpha\phi_v = \mathscr{B}\kappa_1\,, \tag{65}$$

where the kinematic boundary condition (31) is equivalent to (see Tanveer and Saffman[17] for details)

$$\tilde{\psi}_{1_\nu} = y_\nu x_{1_t} - x_\nu y_{1_t}\,, \tag{66}$$

where

$$\kappa_1 = [1/(x_\nu^2+y_\nu^2)^{3/2}]\{y_{\nu\nu}x_{1_\nu} - x_{\nu\nu}y_{1_\nu} + x_\nu y_{1_{\nu\nu}} - y_\nu x_{1_{\nu\nu}} - 3[(x_\nu x_{1_\nu} + y_\nu y_{1_\nu})/(x_\nu^2+y_\nu^2)](x_\nu y_{\nu\nu} - y_\nu x_{\nu\nu})\}\,, \tag{67}$$

$$\tilde{\phi}_1 + i\tilde{\psi}_1 = \tilde{W}_1\,, \tag{68}$$

$$\tilde{x}_1 + i\tilde{y}_1 = \tilde{z}_1\,, \tag{69}$$

$$x_1 + iy_1 = \tilde{z}_1 + z_{0_{\tilde{\beta}}}\beta_1 + (z_{0_{\tilde{\rho}}} + f_{\tilde{\rho}})\rho_1\,, \tag{70}$$

$$x + iy = z_0(\zeta,\rho,\pi) + f(\zeta,\rho)\,, \tag{71}$$

where β_1, ρ_1 are the perturbation of $\tilde{\rho}$ and $\tilde{\beta}$ about the stationary values ρ and π, respectively, and the subscripts $\tilde{\beta}$ and $\tilde{\rho}$ denote derivatives with respect to these two variables at the stationary values.

Now, for the given boundary location of the bubble, it is necessary to determine ϕ_v on the boundary. This is done in the following manner. We note that for a clockwise contour around the bubble boundary in the physical z plane, it follows from Cauchy's integral formula that

$$-\frac{1}{\pi i}\int\frac{\phi_v + i\psi_v}{z'-z}\,dz' = \phi_v + i\psi_v\,, \tag{72}$$

where the quantity $\phi_v + i\psi_v$ inside the integral is evaluated at z', whereas on the rhs of (72), evaluation is at z, which is also a point on the bubble boundary. We substitute for ψ_v from (30). Further, since for the steady state ψ and ϕ_v are each zero on the bubble boundary, it follows that to linear order we can substitute $\psi = \tilde{\psi}_1$ and shift the contour of integration in (72) to the steady bubble boundary which is parametrically described by (71) when $\zeta = e^{i\nu}$ for ν ranging in the interval $[-\pi,\pi]$. We will call this $z_s(\nu)$. Then, z and z' in (72) can be expressed as $z_s(\nu)$ and $z_s(\nu')$, respectively. By taking the real part of (72), we then have a Fredholm integral equation of the second kind for the unknown ϕ_v:

$$\phi_v(\nu) + \frac{1}{\pi}\int_{-\pi}^{\pi}d\nu'\,\phi_v(\nu')K(\nu,\nu') = -\frac{1}{\pi}\int_{-\pi}^{\pi}d\nu'\,\tilde{\psi}_1(\nu')K_1(\nu,\nu')\,, \tag{73}$$

where

$$K(\nu,\nu') = \mathrm{Im}\left(\frac{dz_s}{d\nu}(\nu')\frac{1}{z_s(\nu')-z_s(\nu)}\right) \tag{74}$$

and

$$K_1(\nu,\nu') = \mathrm{Re}\left(\frac{dz_s}{d\nu}(\nu')\frac{1}{z_s(\nu')-z_s(\nu)}\right). \tag{75}$$

We note that $dz_s/d\nu = i\zeta(dz_s/d\zeta)$, which is evaluated by using (58) and (71). We also note that the singularity of the kernel $K(\nu,\nu')$ when $\nu=\nu'$ is removable by a limiting procedure, whereas K_1 is a singular kernel with $K_1 \sim 1/(\nu'-\nu)$ for small $\nu'-\nu$. For numerical purposes of evaluation of the rhs of (73), it is more convenient to rewrite

$$K_1 = \tilde{K}_1 + \tfrac{1}{2}\cot[(\nu'-\nu)/2]\,. \tag{76}$$

From the definition of $\tilde{K}_1$ in (76), it is clear that it is a regular kernel without any singularity. We also note the Hilbert transform properties for any positive integer n:

$$\frac{1}{2\pi}\int_{-\pi}^{\pi} d\nu' \sin n\nu' \cot\frac{\nu'-\nu}{2} = -\cos n\nu\,, \tag{77}$$

$$\frac{1}{2\pi}\int_{-\pi}^{\pi} d\nu' \cos n\nu' \cot\frac{\nu'-\nu}{2} = \sin n\nu\,. \tag{78}$$

Evaluation of the rhs of (73) for a given sine or cosine series representation of $\tilde{\psi}_1$ is carried out numerically by using a quadrature rule for the integrand $\tilde{K}_1\tilde{\psi}_1$ since it is regular. The remaining part is calculated analytically by using the properties (77) or (78). A solution to the Fredholm integral equation (73) is guaranteed to exist since this is equivalent to solving Laplace's equation for ϕ_v inside the steady bubble with specified normal derivatives on its boundary, where the line integral of the normal derivative along the closed boundary in the physical plane is zero. This follows from the assumption that $\tilde{\psi}_1$ is single-valued as we go around the bubble contour. However, the solution is not quite unique. It is defined up to an additive constant which can be arbitrary. For the dynamics, the arbitrary constant is immaterial since this can be clearly absorbed in the term $\tilde{\phi}_1$ in (65) and a specific choice of the constant is made by the numerical procedure described in Sec. V. Thus ϕ_v is determined in terms of $\tilde{\psi}_1$.

Since Im $\tilde{z}_1$ and Im $\tilde{W}_1$ are each zero on $|\zeta| = \tilde{\rho}$, each of these quantities are also zero on $|\zeta| = \rho$ to leading order. Then it follows that for a general disturbance, $\tilde{z}_1$ and $\tilde{W}_1$ each have Laurent series representations of the form

$$b_0 + \sum_{n=1}^{\infty} (b_n\zeta^n + b_n^*\rho^{2n}\zeta^{-n})\,, \tag{79}$$

where b_0 is real. For symmetric disturbances, the b_n are all real and for antisymmetric disturbances, b_0 is zero, while the other b_n are purely imaginary. The function ϕ_v is an even and odd function of ν corresponding to symmetric and antisymmetric disturbances, respectively. From the real and imaginary parts of (79) on $\zeta = e^{i\nu}$, we can express each of $\tilde{x}_1$ and $\tilde{\phi}_1$ in a cosine series for symmetric disturbances and a sine series for the antisymmetric disturbances: For $\tilde{y}_1$ and $\tilde{\psi}_1$, the opposite is true. From the representation of z_0 in terms of ρ and β, it is not difficult to deduce from (65) and (66) that $\beta_1 = 0$ for symmetric disturbances and $\rho_1 = 0$ for antisymmetric disturbances. We now look for normal solutions to (65) and (66). For symmetric disturbances, we have

$$\tilde{x}_1 = e^{\sigma t}\left(c_0 + \sum_{n=1}^{\infty} c_n(1+\rho^{2n})\cos n\nu\right), \tag{80}$$

$$\tilde{y}_1 = e^{\sigma t}\left(\sum_{n=1}^{\infty} c_n(1-\rho^{2n})\sin n\nu\right), \tag{81}$$

$$\tilde{\phi}_1 = e^{\sigma t}\left(d_0 + \sum_{n=1}^{\infty} d_n(1+\rho^{2n})\cos n\nu\right), \tag{82}$$

$$\tilde{\psi}_1 = e^{\sigma t}\left(\sum_{n=1}^{\infty} d_n(1-\rho^{2n})\sin n\nu\right). \tag{83}$$

For antisymmetric disturbances, we have

$$\tilde{x}_1 = e^{\sigma t}\left(\sum_{n=1}^{\infty} c_n(1+\rho^{2n})\sin n\nu\right), \tag{84}$$

$$\tilde{y}_1 = e^{\sigma t}\left(-\sum_{n=1}^{\infty} c_n(1-\rho^{2n})\cos n\nu\right), \tag{85}$$

$$\tilde{\phi}_1 = e^{\sigma t}\left(\sum_{n=1}^{\infty} d_n(1+\rho^{2n})\sin n\nu\right), \tag{86}$$

$$\tilde{\psi}_1 = e^{\sigma t}\left(-\sum_{n=1}^{\infty} d_n(1-\rho^{2n})\cos n\nu\right). \tag{87}$$

In either case, if we truncate the infinite series representation in (80)–(87) and solve for the point values of ϕ_v at uniformly spaced out points in the upper-half semicircular boundary by solving the discretized linear system of equations obtained from (73), we obtain a matrix eigenvalue problem by satisfying (65) and (66) at this discrete set of points. The details are described in Sec. V.

We note that it is not necessary for any eigenvector comprising the components c_n and d_n and ρ_1 or β_1 to be real even though each of the functions $\tilde{x}_1$, $\tilde{y}_1$, $\tilde{\phi}_1$, and $\tilde{\psi}_1$ defined by (68) and (69) and the constants ρ_1 and β_1 are real valued on $\zeta = e^{i\nu}$. This is because for a general time-dependent problem, each of these functions, as well as ρ_1 and β_1, are written as sums over all the eigenfunctions, each of which has the form (80)–(83) or (84)–(87). Although the sum has to be real, each eigenfunction can be complex.

V. NUMERICAL PROCEDURE FOR BUBBLES

For symmetric modes, we truncate expressions (80) and (81) to $N-1$ terms, i.e., we set $c_j = 0$ for $j \geqslant (N-1)$. Equations (82) and (83) are truncated to N terms so that $d_j = 0$ for $j \geqslant N$. The representation (61) is truncated to N_s terms for the coefficients a_n. These have been obtained from previous work on the steady-state bubble.[9] The point values of ϕ_v at $N+1$ points on the upper-half semicircle $\zeta_k = e^{ik\pi/N}$, where k is an integer ranging from 0–N, are expressed in terms of given coefficients d_j in the following manner. Equation (73) is satisfied at these $N+1$ ν points. The integral on the lhs of (73) is approximated by a sum using the point values of the integrand at $2N$ uniformly spaced out points on the unit circle including the $(N+1)$ collocation points. For the integration points on the lower-half semicircle, we use the known symmetry of ϕ_v for evaluation of the integrand. We now evaluate the rhs of (73). The integral of $\tilde{K}_1\tilde{\psi}_1$ is carried out by approximating it as a sum over the $2N$ points, as before. Antisymmetry of $\tilde{\psi}_1$ is used to find the integrand values at points on the lower-half semicircle. The remaining part of the rhs of (73) consists of integrals, as on the lhs of (77), which is found exactly. We then end up with a matrix equation

$$H\boldsymbol{\phi}_v = D\,\mathbf{d}\,, \tag{88}$$

where $\boldsymbol{\phi}_v$ is a column vector of $N+1$ point values of ϕ_v and $\mathbf{d}$ is a column vector with components $(d_0, d_1, \ldots, d_{N-1})$. The matrix H is a square matrix, but D is a $(N+1)\times N$ matrix. Since the homogeneous Fredholm integral equation defined in (73) allows for one and only one linearly independent solution that is identically equal to a constant, it is expected that the discretized version in (88) has the same property, at least for large N. Therefore, the matrix H is expected to be rank deficient by 1 and the column vector with components $(1,1,1,\ldots,1)$ is the one and only independent null vector. Since the solution will be arbitrary to an additive constant, we impose the condition that the sum of all the components

of the vector ϕ_v is zero in order to obtain a unique solution to (88). With this condition, it is clear that any solution $\boldsymbol{\phi}_v$ to (88) will also satisfy

$$(A+\Lambda)\boldsymbol{\phi}_v = D\mathbf{d}\,, \tag{89}$$

where Λ is a matrix with all entries equal to 1. Now, throughout our calculations the matrix $(A+\Lambda)$ was found to be nonsingular, with moderate values of the condition number. Since $A+\Lambda$ is nonsingular, there can be only one solution to (89), which must be the solution to (88) satisfying the constraint on the sum of the components of the solution vector being zero. The system (89) is easily solved numerically by using a standard linear equation solver. With the point values of ϕ_v known in terms of d_j at $N+1$ uniformly spaced out points in the upper-half unit semicircle, (65) and (66) are satisfied at these points. Because of the assumed symmetry, it is not necessary to satisfy (65) and (66) at any points in the lower-half semicircle. We thus obtain a matrix eigenvalue problem of dimension $2N$, where the eigenvector X, written as a column, is given by

$$X^T = (\rho_1, c_0, c_1, c_2, \ldots, c_{N-2}, d_0, d_1, \ldots, d_{N-1})\,. \tag{90}$$

The size of the system is reduced by half by noticing the block structure of the eigenvalue problem given by

$$\begin{pmatrix} A_1 & A_2 \\ -\sigma B_3 & A_4 \end{pmatrix}\begin{pmatrix} X_1 \\ X_2 \end{pmatrix} = 0\,, \tag{91}$$

where $X_1^T = (\rho_1, c_0, \ldots, c_{N-2})$ and $X_2^T = (d_0, \ldots, d_{N-1})$. From (91), we can eliminate X_2 to obtain

$$-B_3^{-1}A_4A_2^{-1}A_1X_1 = \sigma X_1\,, \tag{92}$$

which was solved using a standard eigenvalue solver. Consistency of the eigenvalues and eigenvectors was checked by doubling N. The steady-state truncation N_s was also varied to check the results. We found $N=256$ and $N_s=128$ to be adequate to give at least three-figure accuracy in the eigenvalues for all the branches in the entire range of calculations reported, except when $\mathscr{B} \leqslant 0.002$. For these smaller values of $\mathscr{B}$, $N=512$ and sometimes $N=1024$ were necessary to find at least a two-figure accuracy in the eigenvalues up to $\mathscr{B}=0.0006$, beyond which the calculations were not reliable.

For antisymmetric modes, we truncate the summation in (84) and (85) to $N-1$ terms and we truncate the summation in (86) and (87) to N terms. The lhs of (73) is discretized at N points on the unit semicircle $\zeta_k = e^{i\nu_k}$, where $\nu_k = \pi/(2N) + k\pi/N$, k ranges from 0–$N-1$, and the integral is replaced by a sum of $2N$ uniformly spaced out points on the unit circle that includes the N collocation points. For integration points on the lower-half semicircle, the known symmetry of ϕ_v allows us to express it in terms of the point values of the unknown collocation points. The integral on the rhs of (73) is also calculated using the same discretization points, except that the kernel K_1, as in the symmetric case, is desingularized by subtracting the singularity from the numerical integrand and adding it back analytically by using (78). Once again, we obtain a matrix equation of the form (88), where the matrices H and D are now $N\times N$ square matrices. In this case, the matrix H is nonsingular since the continuum problem has a unique solution. Thus we obtain the relation between the unknown point values of ϕ_v and the coefficients d_j. Equations (65) and (66) are now each satisfied at these N points. The points $\zeta=1$ and $\zeta=-1$ are avoided because (65) and (66) are automatically satisfied at those points for antisymmetric disturbances. Because of the assumed antisymmetry of the disturbance, it is not necessary to satisfy (65) and (66) at ζ points on the lower-half semicircle. Once again, we have a generalized matrix eigenvalue problem of the form of (91), except that $X_1^T = (\beta_1, c_1, \ldots, c_{N-1})$ and $X_2^T = (d_1, \ldots, d_N)$ in this case. It was found that $N=512$ was adequate to give three-figure accuracy for the three smallest eigenvalues over the range of calculations reported. The antisymmetric modes did not appear to be as sensitive to the truncation for small $\mathscr{B}$ as were the symmetric disturbances.

VI. NUMERICAL RESULTS FOR BUBBLES

Using the procedure as described in Sec. V, we calculated the eigenvalues and eigenmodes of the linear stability operator for a wide range of values of surface tension and bubble size and for different values of the viscosity ratio α. Here, all the results presented will be for $\alpha=0.1$. We also present $\alpha=0$ results obtained previously[17] for comparison purposes. For small surface tension, the eigenvalues for any α from numerical calculations appear to be different from the corresponding eigenvalues for zero α by a factor of $1/(1+\alpha)$, in accordance with the analytic theory for the finger described in Sec. VII.

For small sized bubbles on the McLean–Saffman branch, the predictions of the decay rates of the various eigenmodes agreed very well with the analytical prediction (53). Figures 3 and 4 show the eigenvalue corresponding to the least stable symmetric disturbance (other than the translation mode) for $\mathscr{B}$ in different ranges for three different values of the bubble area J; the $\alpha=0$ case is also shown for

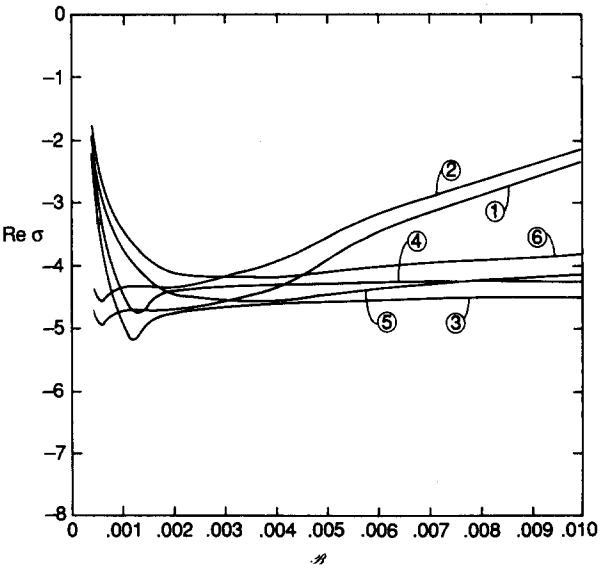

FIG. 3. The growth rate Re σ corresponding to the least stable symmetric nontrivial mode for the McLean–Saffman bubble branch for $\mathscr{B}$ in the interval (0.006,0.01). Curve ①: $J=0.3854$, $\alpha=0$; curve ②: $J=0.3854$, $\alpha=0.1$; curve ③: $J=1.3854$, $\alpha=0$; curve ④: $J=1.3854$, $\alpha=0.1$; curve ⑤: $J=3.8854$, $\alpha=0$; curve ⑥: $J=3.8854$, $\alpha=0.1$.

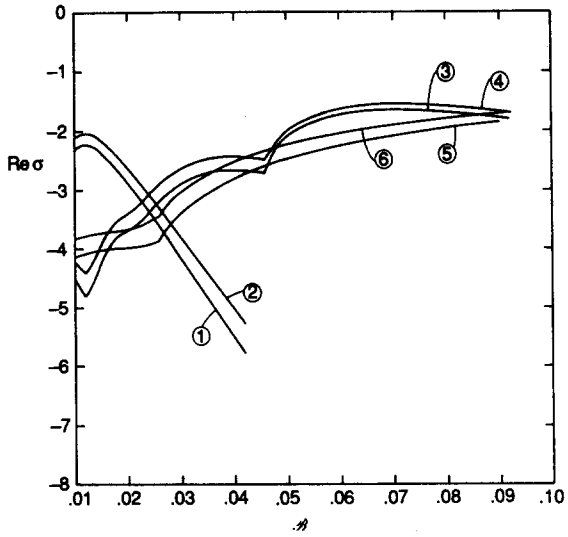

FIG. 4. The growth rate Re σ corresponding to the least stable symmetric nontrivial mode for the McLean–Saffman bubble branch for $\mathscr{B}$ in the interval (0.01,0.092). Curves 1 and 2 are almost straight beyond $\mathscr{B} = 0.042$. The different labels ①–⑥ correspond to the different cases described in Fig. 3.

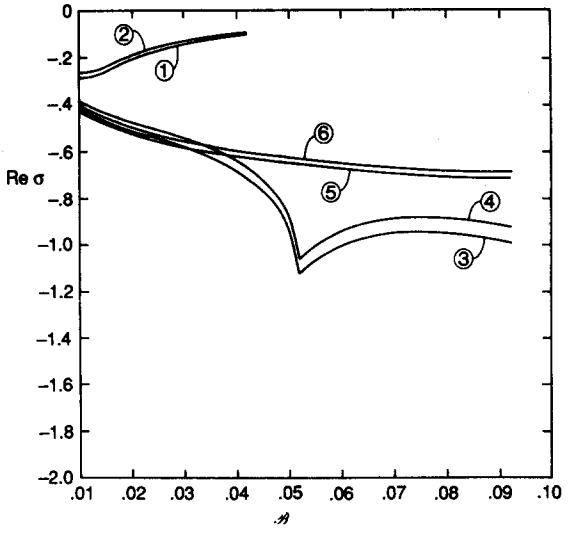

FIG. 6. The growth rate Re σ corresponding to the least stable antisymmetric mode for the McLean–Saffman bubble branch for $\mathscr{B}$ in the interval (0.01,0.092). For the small bubble size, this mode tends to the neutral translation mode in the y direction of the $J \to 0$ limit of Sec. III. The different labels ①–⑥ correspond to the different cases described in Fig. 3.

comparison. Corresponding plots for antisymmetric disturbances are shown in Figs. 5 and 6. The decay rate of these modes is found to be quite dependent on the bubble area since the corresponding modal disturbances affect the sides and back of the steady-state bubble, leaving the front quite unchanged. In the limit of infinite bubble size, i.e., a finger, these modes should correspond to a continuum of modes for which the disturbance advects along the sides.[4] The numerical resolution of eigenmodes and eigenvalues becomes more and more difficult with smaller surface tension, as expected from the properties of the zero surface tension stability operator. However, from extrapolation it appears that the bubble remains stable for any nonzero surface tension, as was concluded previously[17] for the zero viscosity ratio.

Figures 7 and 8 show the growth rate for the unstable symmetric and antisymmetric mode for the first Romero–Vanden-Broeck branch of steady bubble solutions.[9] As in the case of zero α,[17] there is a small range of values of $\mathscr{B}$ where there are two unstable antisymmetric eigenmodes, rather than one for a range of values of area J. For larger values of $\mathscr{B}$, these two modes coalesce to form a complex pair of eigenvalues at points on the curves in Fig. 8 where the slope is discontinuous. The unstable eigenmodes all affect the tip of the bubble, while leaving the rest of the steady bubble quite unaffected. The growth rates for these modes are found to be independent of the bubble size once the bubble is large

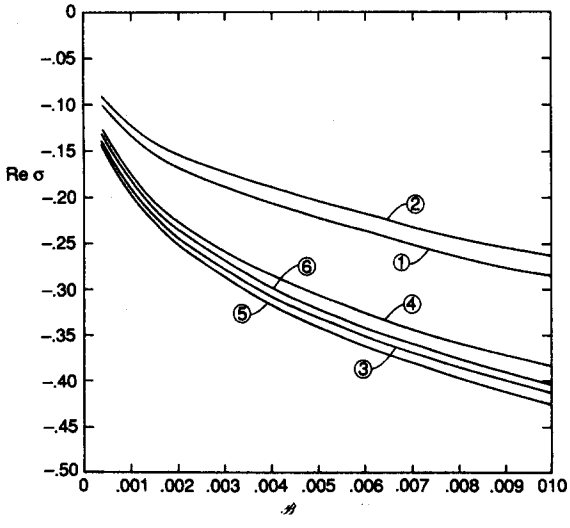

FIG. 5. The growth rate Re σ corresponding to the least stable antisymmetric mode for the McLean–Saffman bubble branch for $\mathscr{B}$ in the interval (0.004,0.01). The different labels ①–⑥ correspond to the different cases described in Fig. 3.

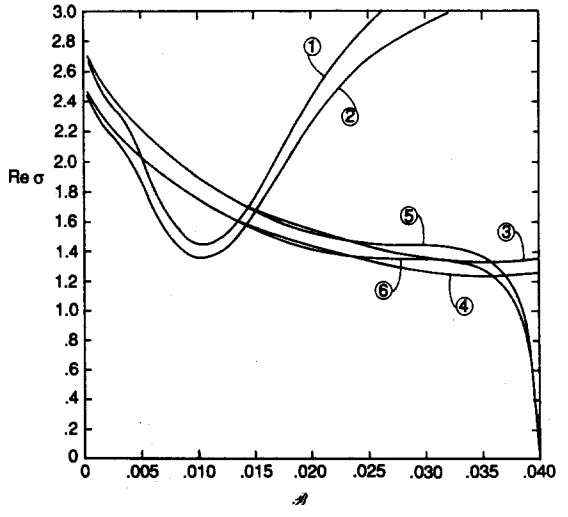

FIG. 7. The growth rate Re σ corresponding to the unstable symmetric eigenmode of the first Romero–Vanden-Broeck bubble solution. In this case σ is always real. The different labels ①–⑥ correspond to the different cases described in Fig. 3.

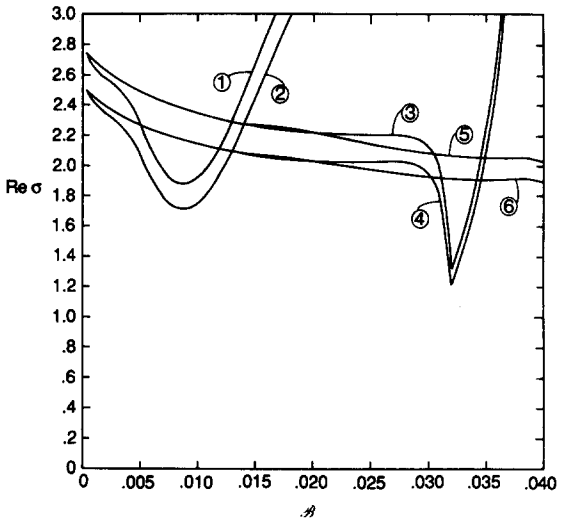

FIG. 8. The growth rate Re σ for the antisymmetric most unstable eigenmode of the first Romero–Vanden-Broeck bubble solution. In this case, for $J = 1.3854$, as shown in curves ③ and ④, σ is complex for $\mathscr{B} > 0.032$ and results from the merger of two real positive eigenvalues existing over some small range of values of $\mathscr{B}$ for $\mathscr{B} < 0.032$. Over most of the range of $\mathscr{B}$, there is only one unstable eigenmode. The labels on the curves are the same as described in Fig. 3.

enough. This suggests that the instability modes persist for the case of a finger on the Romero–Vanden-Broeck branch. Indeed, for small $\mathscr{B}$, our numerical results for the instability mode agree very well with the analytical result

$$\sigma = 2.805/(1+\alpha) + k\mathscr{B}^{2/3} \tag{93}$$

obtained in Sec. VII for the finger; however, the value of k is not determined in Sec. VII. For the bubble, from the slope of the graph of the numerically calculated unstable eigenvalue σ against $\mathscr{B}^{2/3}$ for small $\mathscr{B}$, we find that for $\alpha = 0.1$, k was -19 and -10 for the symmetric and antisymmetric cases, respectively. This turns out to be the same as for $\alpha = 0$ reported previously.[17]

We do not present any calculations for other Romero–Vanden-Broeck branches of solution since, as demonstrated previously[17] for $\alpha = 0$, they are expected to be unstable for nonzero α.

VII. ANALYTIC THEORY FOR THE FINGER

Here, we extend the analytic theory for the stability of fingers[16] to include the finite viscosity ratio effect. Rather than repeat all the details of Ref. 16, which are quite messy, we will just denote what steps do or do not require modification. We are assuming the reader is familiar with the content of Ref. 16; the notation in this section is the same as in that paper. Unfortunately, there is some conflict with the notation in Secs. III–V of this paper that we could not avoid. Since this section is totally independent of Secs. III–V, there should be no confusion. Any reference to the equations of Ref. 16 will begin with letter "t"; for example, (t29) refers to Eq. (29) of Ref. 16.

As in Ref. 16, we introduce a unit semicircle as the work plane, called the ζ plane, where the circular part of the boundary corresponds to the boundary of the finger and the diameter corresponds to the walls of the cell. Equations (t1)–(t6) remain unchanged, except that U is now the equivalent velocity ratio defined by (24). Equation (t7) has to be replaced by (27). We now define an analytic function $\tilde{\chi}(\zeta)$ inside the unit semicircle such that on the real diameter of the unit semicircle in the ζ plane,

$$\operatorname{Im} \tilde{\chi}(\zeta) = 0\,, \tag{94}$$

and on the arc of the unit semicircle,

$$\operatorname{Re} \tilde{\chi}(\zeta) = (\pi\lambda/2)\,\phi_v\,, \tag{95}$$

where ϕ_v is evaluated at the z point of the finger boundary determined by the conformal map $z(\zeta)$ that maps the unit semicircle into the flow domain exterior of the finger. Note that $(2/\pi\lambda)\tilde{\chi}$ is not equal to $\phi_v + i\psi_v$ since the latter is analytic and free of singularities inside the finger, while $\tilde{\chi}$ is analytic outside. The term $\tilde{f} + \tilde{W}$ on the lhs of (t8) has to be replaced by $\tilde{f} + \tilde{W} - \tilde{\alpha}\chi$ and $\mathscr{G}$ has to be redefined as $\pi^2\mathscr{B}/(4U)$. Equations (t9)–(t18) remain unchanged. In addition to (t18), since for the steady state $\tilde{\chi} = 0$, the perturbation is of order ϵ and we define χ:

$$\tilde{\chi} = \epsilon\chi\,. \tag{96}$$

The $F + w$ on the lhs of (t19) has to be replaced by $F + w - \alpha\chi$.

In the next step, in the Tanveer[16] paper, a zero surface tension analysis was carried out to show that the stability operator in that case has a continuous spectrum with Re $\sigma \geqslant 0$. Explicit integral expressions for the modes were obtained. In Sec. IV of Ref. 16, it was shown that a regular perturbation expansion in powers of $\mathscr{G}$ can be carried out without any further restrictions on σ. Here, we are unable to calculate explicitly the zero surface tension modes for arbitrary α. However, it appears that for small α, a perturbation expansion of the zero surface tension modes can be carried out in principle without any further restriction of σ. We will assume here that there exist zero surface tension eigenmodes for nonzero α for Re $\sigma \geqslant 0$ and that a regular perturbation expansion of these modes in powers of surface tension can be constructed for the small surface tension without any restriction on σ. Thus we are assuming that the restrictions on the spectrum arise only as a result of transcendentally small terms in surface tension, as has been shown previously[16] for the case of zero α. There is indirect evidence to suggest that this is a correct assumption, since the predictions of the eigenvalues based on the calculation of transcendentally small terms is found to be in agreement with the numerically calculated eigenvalues of the stability operator for large bubbles for eigenmodes that only affect the front of the bubble.

Following the procedure of the Tanveer[16] paper for the determination of the transcendental terms described in Sec. V, we analytically continue the equations to the ζ plane outside the unit circle in the upper-half plane. In lieu of $\tilde{W}$ in Eqs. (t45), (t46), and (t51), we use $\tilde{W} - \alpha\tilde{\chi}$. All the other equations from (t44)–(t62) are valid without any change. The variables w in (t63), (t71), (t81), and (t82) have to be replaced by $w - \alpha\chi$, while all the other equations from (t63)–(t85) remain valid without any change. Now, we need a relation between χ and w to proceed any further. This

is done by noticing from Cauchy's integral formula that, for z outside the finger,

$$\int \frac{\phi_v + i\psi_v}{z' - z}\, dz' = 0\,, \tag{97}$$

where the contour of integration is along the finger boundary starting from $y = \lambda$ and ending at $y = -\lambda$. From (30), we can replace ψ_v in (97) by ψ. Again, since the finger boundary is assumed to be analytic, each of the functions ϕ_v and ψ possess harmonic continuation outside and inside the finger, respectively. Thus, for small disturbances, the contour of integration in (97) can be changed from the instantaneous finger boundary to the steady finger boundary. It is convenient to use the conformal mapping function $z_s(\zeta)$ that maps the interior of the unit semicircle in the ζ plane to the flow domain exterior of the steady finger, with $\zeta = e^{i\nu}$ for ν in $(0,\pi)$ corresponding to the finger boundary. From (t3), we have $z_s = z_0 + (2/\pi) f$, where f is determined from (t16) and

$$z_0(\zeta) = -(2/\pi)(1-\lambda)\ln\zeta + (2/\pi)[\ln(\zeta - 1) + \ln(\zeta + 1)]\,. \tag{98}$$

For ζ inside the unit semicircle, using the definition of χ from (94)–(96) and of w from (t5) and (t18), Eq. (97) implies

$$\frac{1}{2\pi i}\int_C \frac{\chi(\zeta') + \chi(1/\zeta')}{z_s(\zeta') - z_s(\zeta)}\frac{dz_s}{d\zeta'}\,d\zeta' = -\frac{1}{2\pi i}\int_C \frac{w(\zeta') - w(1/\zeta')}{z_s(\zeta') - z_s(\zeta)}\frac{dz_s}{d\zeta'}\,d\zeta'\,, \tag{99}$$

where the contour C in the above integrals in the ζ' plane coincides with the arc of the semicircle from $+1$ to -1. The lhs of Eq. (99) will be defined to be $I_6(\chi, z_s, \zeta)$ and the rhs will be defined to be $I_7(w, z_s, \zeta)$. By the contour deformation technique employed previously,[16] it is clear that for $|\zeta| > 1$, the analytic continuation of (99) gives us

$$\chi(\zeta) = -w(\zeta) - \chi(1/\zeta) + w(1/\zeta) + I_7 - I_6\,. \tag{100}$$

We note that I_7 and I_6 will be finite for $|\zeta| > 1$ provided $z_s(\zeta) \neq z_s(\zeta')$. Now for $\mathcal{G} = 0$, $z_s = z_0$, as given by (98). For $\lambda = \frac{1}{2}$, which is the selected value in the limit of zero surface tension, it is easily shown from (98) that indeed for $|\zeta| > 1$, $z_0(\zeta) \neq z_0(\zeta')$ since ζ' by definition is on the unit semicircular boundary. In this case, we see that I_6 and I_7 are analytic as well outside the unit circle. For nonzero, but small surface tension, it has been shown earlier[16] that the function f, the deviation of z_s from z_0, scales as $\mathcal{G}^{2/3}$ in the vicinity of the singular points at $\zeta = \pm 1/p$ and is of order $\mathcal{G}$ near the unit semicircular boundary. Again the deviation of λ from one-half also scales as $\mathcal{G}^{2/3}$. Thus, from Rouche's theorem, it should be possible to rigorously prove that for ζ outside the unit circle $z_s(\zeta) \neq z_s(\zeta')$ and so each of I_6 and I_7 are finite. However, we do not attempt any such proof here. Thus, from (100), it is clear that in the immediate vicinity of $\zeta = \pm 1/p$, the leading-order behavior of χ is given by w plus some constant since $w(1/\zeta)$ and $\chi(1/\zeta)$ are analytic and free of singularities for $|\zeta| > 1$. Thus, in Eq. (t81), w on the lhs can be replaced by $w(1+\alpha)$, rather than $w - \alpha\chi$, as mentioned earlier, except that the rhs is now modified. It is easy to see that to leading order the rhs will now scale as p^2 as before and there will be additional contributions to R_4 from I_6 and I_7. This additional contribution has no bearing in the determination of the limiting value of σ as the surface tension tends to zero, but appears in the next-order correction in the surface tension for the eigenvalue, which in the case of the nonzero limiting eigenvalue will still be of the form (t104), implying a $\mathcal{G}^{2/3}$ power law dependence, as has been verified by numerical calculations for large bubbles. With the changed definition of R_4 and hence R in (t87) and (t92), we obtain exactly the same equation, except σ is now replaced by $\sigma(1+\alpha)$. Equations (t85) and (t86) hold as is. Equations (t96) and (t97) are not valid here since we do not know the zero surface tension modes. However, it is clear that the zero surface tension modes must behave algebraically and that (t95) must match with the zero surface tension modes for some choice of the constant C_1. Thus to leading order, we end up with

$$\omega''' + P\omega'' + Q\omega' + \sigma(1+\alpha)L\omega = 0\,, \tag{101}$$

which is exactly the same as (t98) except that σ is now replaced by $\sigma(1+\alpha)$. It is therefore clear that if σ_0 is the limiting growth rate for any modes for the problem with zero viscosity ratio, the growth rate in this case will only be different by a factor of $1/(1+\alpha)$, which is consistent with numerical results for bubbles presented in Sec. VI for modes that affect only the front of the bubble. After each occurrence of σ is replaced by $(1+\alpha)\sigma$, the remainder of the Tanveer[16] paper requires no additional modification.

Thus the limiting value of σ as the surface tension tends to zero is only modified by a constant multiple and none of the qualitative conclusions reached in the Tanveer[16] paper is changed by the effect of the finite viscosity ratio. For the unstable modes affecting the first Romero–Vanden-Broeck branch of bubble solutions, noting the differing definition of σ between Sec. VI and the present section, we arrive at formula (93). We do not determine the numerical value of the coefficient k in this paper since it involves a large amount of algebra.

VIII. CONCLUSION

We have incorporated the finite viscosity ratio effect on the stability of fingers and bubbles in a Hele–Shaw cell and find that the finite viscosity ratio does not change any of the qualitative conclusions on stability reached previously for the zero viscosity case.[4,13–17] From a mathematical standpoint, the construction of an analytic theory for the determination of the eigenvalues of the linearized stability operator is, we believe, quite significant in this problem since unlike the case of the zero viscosity ratio, we do not have closed form expressions for the eigenmodes for zero surface tension. This may have direct bearing in problems such as directional solidification, where there exists no known closed form solutions even for zero surface tension and for an advancing solid–liquid interface. This has been generally perceived to be a major stumbling block in the construction of an analytic theory for the directional solidification problem.

ACKNOWLEDGMENT

This research has been supported by National Science Foundation Grant No. DMS-8713246.

[1]P. G. Saffman, J. Fluid Mech. **173**, 73 (1986).
[2]D. Bensimon, L. P. Kadanoff, S. Liang, B. I. Shraiman, and C. Tang, Rev. Mod. Phys. **58**, 977 (1986).
[3]G. M. Homsy, Annu. Rev. Fluid Mech. **19**, 271 (1987).
[4]D. Kessler and H. Levine, Phys. Rev. A **33**, 2621, 2634 (1986).
[5]R. Combescot, T. Dombre, V. Hakim, Y. Pomeau, and A. Pumir, Phys. Rev. Lett. **56**, 2036 (1986).
[6]D. C. Hong and J. S. Langer, Phys. Rev. Lett. **56**, 2032 (1986).
[7]B. I. Shraiman, Phys. Rev. Lett. **56**, 2028 (1986).
[8]S. Tanveer, Phys. Fluids **29**, 3537 (1986).
[9]S. Tanveer, Phys. Fluids **30**, 651 (1987).
[10]S. Tanveer, Phys. Fluids **30**, 1589 (1987).
[11]R. Combescot and T. Dombre, submitted to Phys. Rev. A.
[12]S. Tanveer, submitted to Stud. Appl. Math.
[13]D. Kessler and H. Levine, Phys. Rev. A **32**, 1930 (1985).
[14]D. Kessler and H. Levine, Phys. Fluids **30**, 1246 (1987).
[15]D. Bensimon, Phys. Rev. A **32**, 1302 (1986).
[16]S. Tanveer, Phys. Fluids **30**, 2318 (1987).
[17]S. Tanveer and P. G. Saffman, Phys. Fluids **30**, 2624 (1987).
[18]D. Bensimon, P. Pelce, and B. Shraiman, J. Phys. (Paris) **48**, 1281 (1958).
[19]P. G. Saffman and G. I. Taylor, Proc. R. Soc. London Ser. A **245**, 312 (1958).
[20]G. I. Taylor and P. G. Saffman, Q. J. Mech. Appl. Math. **12**, 265 (1959).
[21]L. P. Kadanoff (private communication).
[22]P. Tabeling, G. Zocchi, and A. Libchaber, J. Fluid Mech. **177**, 67 (1987).
[23]J. W. McLean and P. G. Saffman, J. Fluid Mech. **102**, 455 (1980).
[24]C. W. Park and G. M. Homsy, J. Fluid Mech. **139**, 291 (1983).
[25]D. A. Reinelt, J. Fluid Mech. **183**, 219 (1987).
[26]D. A. Reinelt, Phys. Fluids **30**, 2617 (1987).
[27]S. Sarkar and D. Jasnow, Phys. Rev. A **35**, 4900 (1987).
[28]T. Maxworthy, J. Fluid Mech. **173**, 95 (1986).
[29]A. Kopf-Sill and G. M. Homsy, Phys. Fluids **31**, 18 (1988).
[30]A. J. DeGregoria and L. W. Schwartz, J. Fluid Mech. **164**, 383 (1986).
[31]L. Romero, Ph.D. thesis, California Institute of Technology, 1982.
[32]J. M. Vanden-Broeck, Phys. Fluids **26**, 2033 (1983).
[33]Experiments of Kopf-Sill and Homsy[29] suggest that $U<1$ is possible for bubbles. However, we believe that this is an effect of the differing wetting conditions between the front and back of the bubble.